CRISPR/Cas9-mediated therapeutic effects in Huntington's disease mice

Su Yang[1#], Renbao Chang[1,2,3#], Huiming Yang[1], Ting Zhao[1], Yan Hong[1], Ha Eun Kong[1], Xiaobo Sun[4], Zhaohui Qin[5], Peng Jin[1], Shihua Li[1*] & Xiao-Jiang Li[1,6*]

[1]Department of Human Genetics, Emory University School of Medicine, Atlanta, GA 30322.

[2]Institute of Genetics and Developmental Biology, Chinese Academy of Sciences, Beijing, China 100101

[3]University of Chinese Academy of Sciences, Beijing, China 100039

[4]Department of Mathematics & Computer Sciences, Emory University, Atlanta, GA 30322.

[5]Department of Biostatistics and Bioinformatics, Rollins School of Public Health, Emory University, Atlanta, GA, 30322.

[6]Guangdong-Hongkong-Macau Institute of CNS Regeneration, Ministry of Education CNS Regeneration Collaborative Joint Laboratory, Jinan University, Guangzhou, 510632.

# The first two authors contributed equally to this work.

* Corresponding authors:

Xiao-Jiang Li, 347 Whitehead Building, 615 Michael Street, Atlanta, GA 30322; Tel: 404-727-3290; Email: xli2@emroy.edu

Shihua Li, 346 Whitehead Building, 615 Michael Street, Atlanta, GA 30322; Tel: 404-712-2304; Email: sli@emroy.edu

Conflict of interest: The authors have declared that no conflict of interest exists.

Supplemental Information

Methods

Reagents and antibodies

The anti-huntingtin antibodies (mouse mEM48, which targets amino acid VA residues after the polyQ and polyproline repeats in human exon1 huntingtin) were produced previously in our laboratory (1). Additional antibodies used were HTT (Millipore, MAB2166), 1C2 (Millipore, MAB1574), Tubulin (Sigma, T6557), Vinculin (Sigma, V9131), RFP (MBL, PM005), NeuN (Millipore, MAB377), GFAP (Millipore, AB5804), and Cas9 (Millipore, MAC133).

CRISPR/Cas9-related viral vectors (PX551, PX552) were obtained from Addgene (plasmids #60957 and 60958). AAV-Htt-gRNAs were generated by inserting gRNAs into PX552 via SapI restriction sites. gRNA sequences are as follows: T1: GGCCTTCATCAGCTTTTCCAggg, T2: GGAAGGACTTGAGGGACTCGAagg, T3: GGCTGAGGAAGCTGAGGAGGcgg, T4: GCCCCCGCCGCCACCCGGCCcgg, and control gRNA: ACCGGAAGAGCGACCTCTTCT (PAM sequence are shown in lowercase). AAV-CMV-Cas9 vector was generated by replacing Mecp2 promoter (228 bp) in PX551 with CMV promoter (658 bp) using XbaI and AgeI restriction sites. These viral vectors were sent to the Viral Vector Core at Emory University for packaging and purification of viruses. The genomic titer of viruses was determined by PCR method.

Mice and stereotaxic surgery

All animal procedures were approved by the Institutional Animal Care and Use Committee of Emory University. Full-length mHTT knock-in (CAG140) mice were provided by Dr. Michael Levine at UCLA (2) and were maintained in the animal facility at Emory University in accordance with institutional guidelines.

Stereotaxic surgery was performed as described before (3). Briefly, the mice were anesthetized with 1.5% isoflurane inhalation and stabilized in a stereotaxic instrument (David Kopf Instruments). All

surgical procedures were performed in a designated procedure room and in accordance with the Guidelines for the Care and Use of Laboratory Animals and biosafety procedures at Emory University. Viruses expressing gRNA and Cas9 were mixed at a ratio of 1:4, 1 or 2.5 microliters of the mixed viruses (10^{13} particles/μl) were injected into one side of the mouse striatum according to the following coordinates adjusted to the flat skull position: 0.55 mm rostral to bregma, 2.0 mm lateral to the midline, at 3.5 mm ventral from the dural surface over a period of 5 min using a 28-gauge guide cannula and a 33-gauge injector (Plastics One Inc., Roanoke, Virginia, USA) connected to a Hamilton syringe and a syringe infusion pump (World Precision Instruments, Inc., Sarasota, Florida, USA). Small holes were drilled in the skull, and a 30-gauge Hamilton microsyringe was used to deliver the virus at a speed of 200 nl per min. Meloxicam (2 mg/kg) was given as an analgesic, and after surgery the mice were placed on a heated blanket to recover from the anesthetic.

Mouse behavioral analysis

HD140Q KI mice were bred to generate age-matched homozygous and heterozygous KI mice. HD mice at the age of 9 months were then selected for investigation because these mice show obvious mHTT aggregates and more obvious phenotypes. For behavioral analysis, mice were randomly assigned to the experimental groups, and the tests were performed by a personnel blind to the experimental groups. Mouse body weight was measured weekly, and survival was monitored regularly. The motor function of the mice was assessed with the rotarod test (Rotamex, Columbus Instruments). Mice were trained on the rotarod at 5 RPM for 10 min on 3 consecutive days. After training, the mice were tested for 3 consecutive days, 3 trials per day. The rotarod gradually accelerated to 40 RPM over a 5-min period. Latency to fall was recorded for each trial. The balance beam test was run using a 0.6-cm thick meter stick suspended from a platform on both sides by metal grips. The total running distance was roughly 0.8 m. There was a bright light at the starting point and a dark box at the endpoint. Prior to data collection, each mouse was trained for 3 consecutive days with 3 runs per day. Grip strength was evaluated as described previously (4). Mice were allowed to grip the metal grids of a

grip meter (Ametek Chatillon) with all their limbs, and they were gently pulled backwards by the tail until they could no longer hold the grids. The peak grip strength observed in 5 trials was recorded.

Cell culture

HEK293 cells (ATCC, CRL-1573) were cultured in Dulbecco's modified Eagle's medium supplemented with 10% FBS, 100 µg/mL penicillin, 100 units/mL streptomycin, and 250 µg/µL fungizone amphotericin B. Cells were incubated at 37ºC in 5% CO_2. At a confluency of 70%, the cells were transfected with 1-2 µg/well (6-well plate) or 0.5-1 µg/well (12-well plate) of DNA and lipofectamine (Invitrogen) for 48 h.

Immunohistochemistry

We used a previously described method for immunohistochemistry. Mice were anesthetized and perfused intracardially with 0.9% saline solution for 30 s, followed by 4% paraformaldehyde in 0.1 M phosphate buffer (PB) at pH 7.2. Brains were removed, cryoprotected in 30% sucrose at 4°C, and sectioned at 40 µm using a freezing microtome. Free-floating sections were fixed in 4% paraformaldehyde in 0.1 M phosphate buffer for 10 min and preblocked in 4% normal goat serum in PBS, 0.1% Triton X, and then incubated with primary antibodies at 4°C overnight. The immunoreactive product was visualized with the Avidin–Biotin Complex kit (Vector ABC Elite, Burlingame, CA, USA).

Cultured cells were fixed with 4% paraformaldehyde for 15 min, and then blocked for 1 h with 3% BSA and 0.2% triton X-100 in 1X PBS. Cells were incubated overnight with primary antibodies in 3% BSA in 1X PBS. Fluorescent images were obtained using a Zeiss microscope (Axiovert 200 MOT) with a digital camera (Hamamatsu Orca-100) and Openlab software (Improvision Inc.).

Whole genome sequencing analysis

Genomic DNA extracted from mouse striatum was sent to Novogene for library preparation and whole genome sequencing. For analysis, the 272 bp mouse *Htt* genomic sequence from 34761936 bp to

34762207 bp in chromosome 5 (mm10) was swapped with the 605 bp human *HTT* genomic sequence used to generate HD140Q KI mouse model. The edited mouse genome was used to produce a custom-made index file, and then PEMapper was used to map sequencing data to the custom-made index file. For each on-target and off-target locus, 1 kb of flanking region to each side of the locus was added. We next used the pileup file generated by PEMapper to retrieve the basepair-level sequencing read coverage and reported the average. Top 20 off-target loci were picked by blasting the Htt-gRNAs sequences in mouse genome.

Stereology of mouse striatal volume

Mouse brains were cut into 25 μm serial coronal sections, and every 10th section was used for stereology analysis. The brain sections were stained with cresyl violet acetate solution (Nissl staining). StereoInvestigator software (MBF Bioscience) was used to measure the area of the striatum in each brain section, and to estimate the striatal volume based on the section thickness and number of sections analyzed, with its built-in Cavalieri probe.

Histological quantification

To measure NeuN and GFAP immunostaining intensity, ImageJ software was used. Colored images were first converted to 8-bit black-and-white images. The “Threshold” function was used to adjust the background to highlight NeuN- and GFAP-specific staining. The same threshold was applied to all images analyzed. Finally, the “Measure” function was used to quantify NeuN and GFAP staining intensity in each image.

Western blot

Mouse brain tissues or harvested cells were lysed in ice-cold RIPA buffer (50 mM Tris, pH 8.0, 150 mM NaCl, 1 mM EDTA pH 8.0, 1 mM EGTA pH 8.0, 0.1% SDS, 0.5% DOC, and 1% Triton X-100) containing Halt protease inhibitor cocktail (Thermo Scientific) and PMSF. The lysates were incubated

on ice for 30 min, sonicated, and centrifuged at top speed for 10 min. The supernatants were subjected to SDS-PAGE, and then transferred to a nitrocellulose membrane, which was blocked with 5% milk/PBS for 1 h at room temperature. The blot was incubated with primary antibodies in 3% BSA/PBS overnight at 4°C. After three washes in PBS, the blot was incubated with HRP-conjugated secondary antibodies in 5% milk/PBS for 1 h at room temperature. After three washes in PBS, ECL Prime (GE Healthcare) was then used to detect immunoreactive bands on the blot.

Reference

1. Wang, C.E., Zhou, H., McGuire, J.R., Cerullo, V., Lee, B., Li, S.H., and Li, X.J. 2008. Suppression of neuropil aggregates and neurological symptoms by an intracellular antibody implicates the cytoplasmic toxicity of mutant huntingtin. *J Cell Biol* 181:803-816.
2. Hickey, M.A., Kosmalska, A., Enayati, J., Cohen, R., Zeitlin, S., Levine, M.S., and Chesselet, M.F. 2008. Extensive early motor and non-motor behavioral deficits are followed by striatal neuronal loss in knock-in Huntington's disease mice. *Neuroscience* 157:280-295.
3. Yang, S., Huang, S., Gaertig, M.A., Li, X.J., and Li, S. 2014. Age-dependent decrease in chaperone activity impairs MANF expression, leading to Purkinje cell degeneration in inducible SCA17 mice. *Neuron* 81:349-365.
4. Huang, S., Yang, S., Guo, J., Yan, S., Gaertig, M.A., Li, S., and Li, X.J. 2015. Large Polyglutamine Repeats Cause Muscle Degeneration in SCA17 Mice. *Cell Rep* 13:196-208.

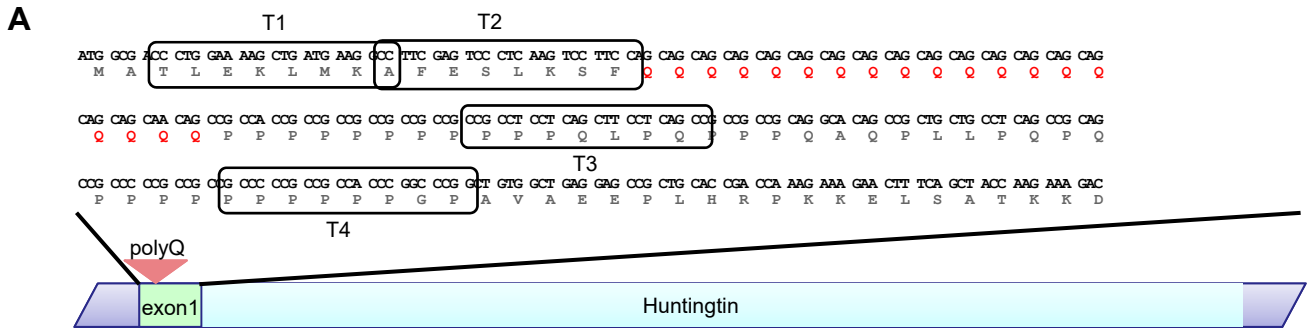
A
T1
T2
T3
T4
polyQ
exon1
Huntingtin

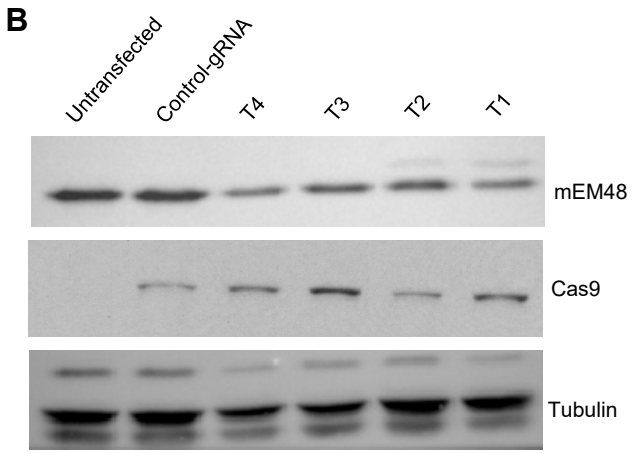
B
Untransfected
Control-gRNA
T4
T3
T2
T1
mEM48
Cas9
Tubulin

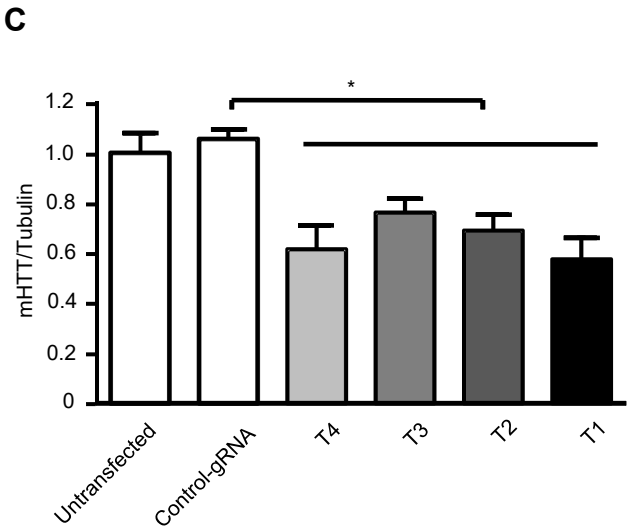
C
mHTT/Tubulin
1.2
1.0
0.8
0.6
0.4
0.2
0
*
Untransfected
Control-gRNA
T4
T3
T2
T1

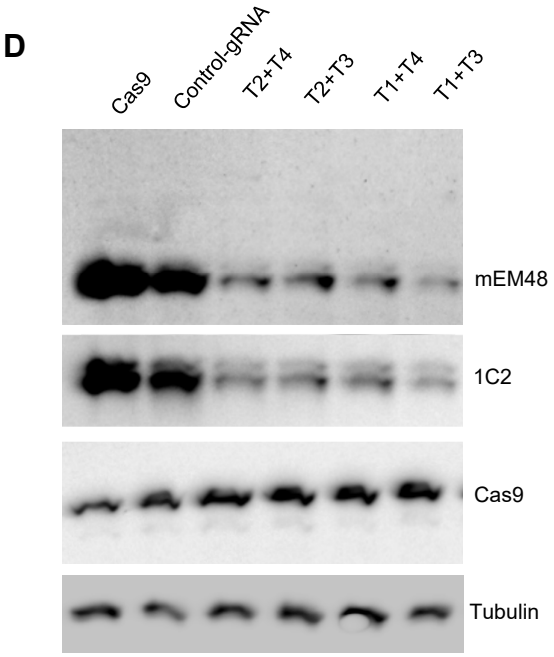
D
Cas9
Control-gRNA
T2+T4
T2+T3
T1+T4
T1+T3
mEM48
1C2
Cas9
Tubulin

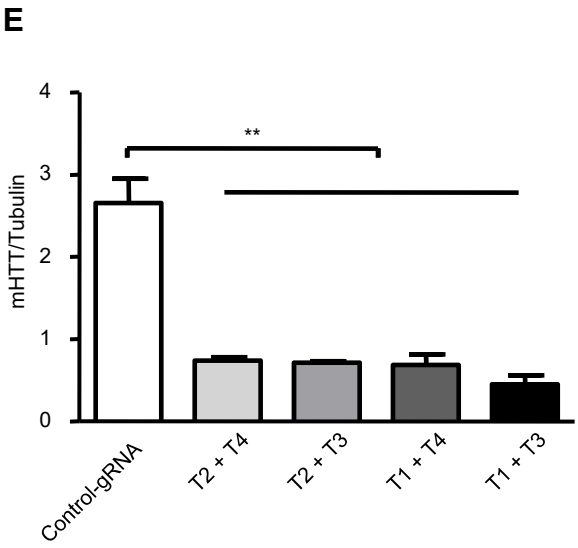
E
mHTT/Tubulin
4
3
2
1
0
**
Control-gRNA
T2 + T4
T2 + T3
T1 + T4
T1 + T3

Supplemental Figure 1. *In vitro* verification of designed Htt-gRNAs (related to Figure 1).

(A) HTT-gRNAs (T1, T2, T3, and T4) were designed to target the regions flanking the polyQ region.

(B) Stable HEK293 cells expressing the exon 1 of human *HTT* with 120 CAG repeats were transfected with each of the designed Htt-gRNAs (T1, T2, T3, and T4) and Cas9. Western blotting analysis showed reduced expression of mutant HTT by Htt-gRNAs, but not Control-gRNA.

(C) Quantitative analysis of the ratio of mEM48-reactive band to tubulin on western blots in Supplemental Figure 1B (n = 3, one-way ANOVA with Tukey tests, * $P < 0.05$).

(D) Stable HEK293 cells expressing the exon 1 of human *HTT* with 120 CAG repeats were transfected with different combinations of two designed Htt-gRNAs (T2+T4, T2+T3, T1+T4, T1+T3) and Cas9. Western blotting analysis showed reduced expression of mutant HTT by Htt-gRNAs, but not Control-gRNA or Cas9 only.

(E) Quantitative analysis of the ratio of mEM48-reactive band to tubulin on western blots in Supplemental Figure 1D (n = 3, one-way ANOVA with Tukey tests, ** $P < 0.01$).

Supplemental Figure 2

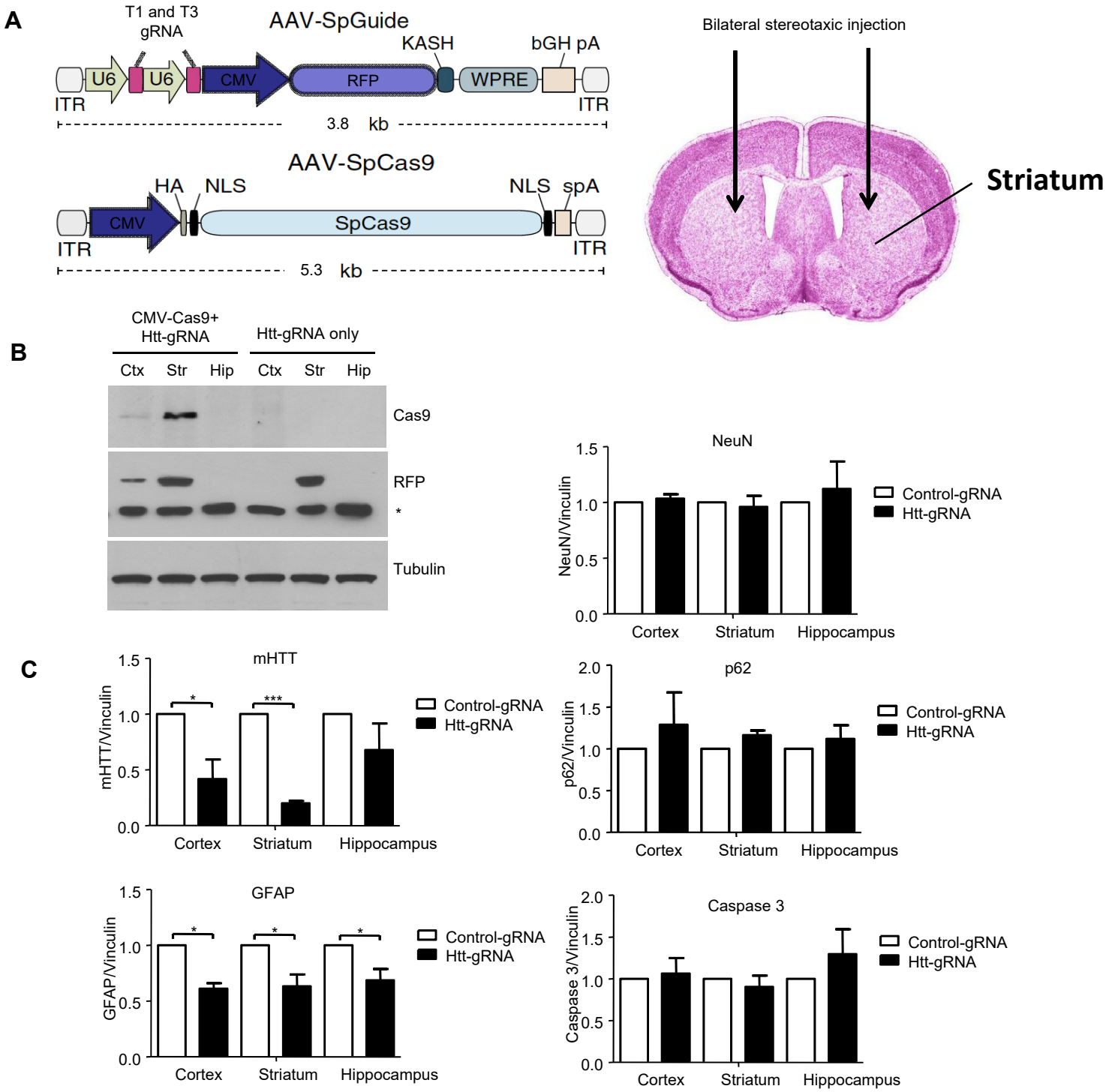

Supplemental Figure 2. Stereotaxic injection of CRISPR/Cas9 viruses into mouse striatum (related to Figure 1).

(A) A schematic representation of AAV-Htt-gRNA and AAV-CMV-Cas9 constructs that were used for stereotaxic injection into the mouse striatum.

(B) Western blot showing the expression of CMV-Cas9 and Htt-gRNA (indicated by the co-expressed RFP) in the injected mouse brain regions. Brain injected with AAV-Htt-gRNA only was used as controls. Replicate samples run on separated blots are presented. The asterisk was used to indicate a non-specific band.

(C) Quantitative analysis of western blotting result in Figure 1C (n = 3, Student's t-test, * $P < 0.05$, *** $P < 0.001$).

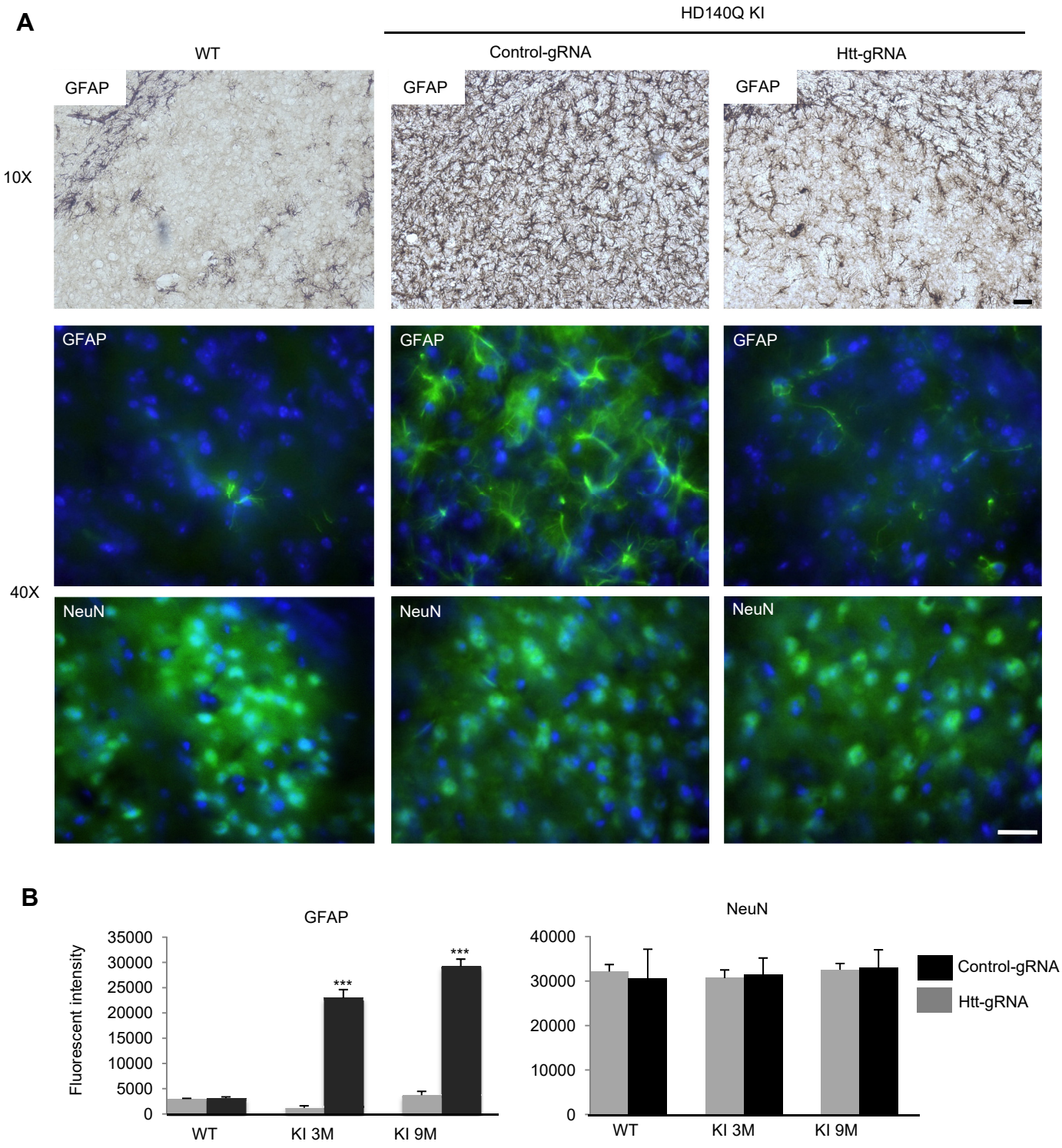
A
HD140Q KI
WT
Control-gRNA
Htt-gRNA
GFAP
10X
40X
NeuN
B
GFAP
Fluorescent intensity
35000
30000
25000
20000
15000
10000
5000
0
***
***
WT
KI 3M
KI 9M
NeuN
40000
30000
20000
10000
0
Control-gRNA
Htt-gRNA

Supplemental Figure 3. Removal of mHTT alleviates neuropathology in homozygous HD140Q KI mouse striatum (related to Figure 1).

(A) Nine-month old homozygous HD140Q KI mice were injected with AAV-Htt-gRNA/AAV-CMV-Cas9 or AAV-Control-gRNA/AAV-CMV-Cas9. Immunostaining analysis of the striatum was done three weeks after injection. Untreated WT mouse striatum served as a control to show the increased GFAP staining in homozygous HD140Q KI striatum, whereas GFAP staining was diminished in the AAV-Htt-gRNA/AAV-CMV-Cas9 injected KI striatum. No difference in NeuN staining was found. Scale bars: 20 μm.

(B) Quantitative analysis of the fluorescent intensity of GFAP and NeuN staining. The striatum of nine-month old untreated WT mice and three or nine-month old homozygous HD140Q KI mice injected with AAV-Htt-gRNA/AAV-CMV-Cas9 or AAV-Control-gRNA/AAV-CMV-Cas9 was analyzed three weeks after injection (n = 4 to 6 mice per group, Student's t-test, *** $P < 0.001$)

Supplemental Figure 4

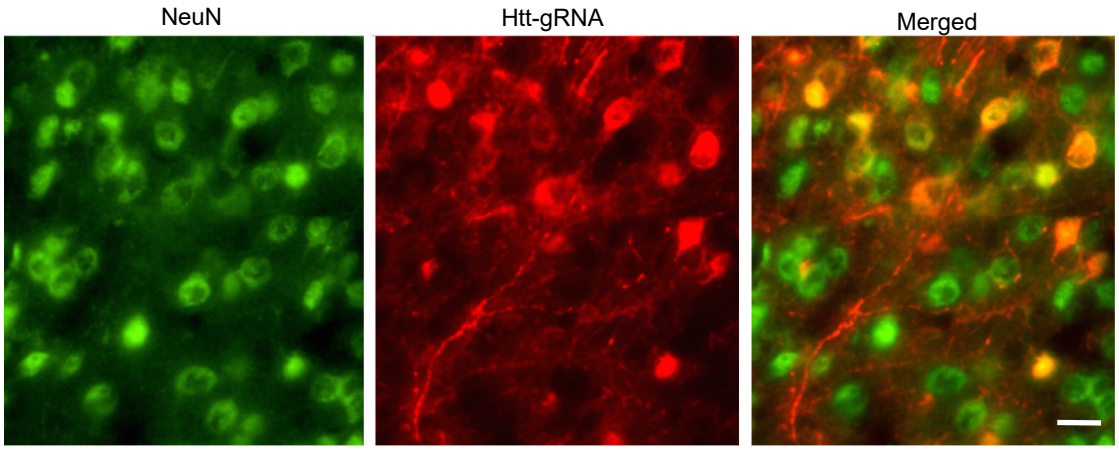

Supplemental Figure 4. Htt-gRNA expression in neuronal cells in the injected striatum (related to Figure 2).

Double immunostaining verified that NeuN-positive cells had been transduced by AAV-Htt-gRNA. Scale bar: 10 μm.

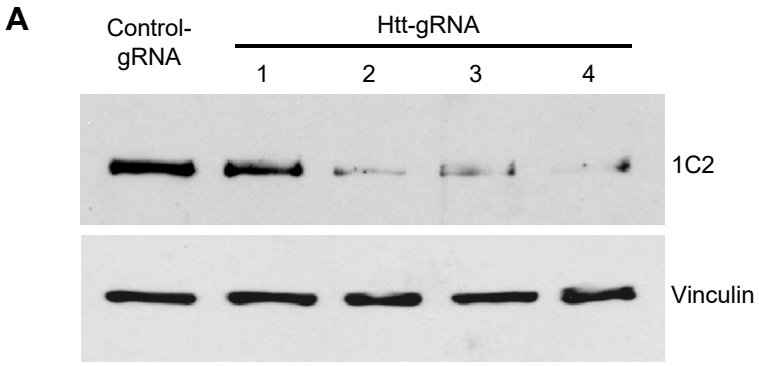
A
Control-
gRNA
Htt-gRNA
1
2
3
4
1C2
Vinculin

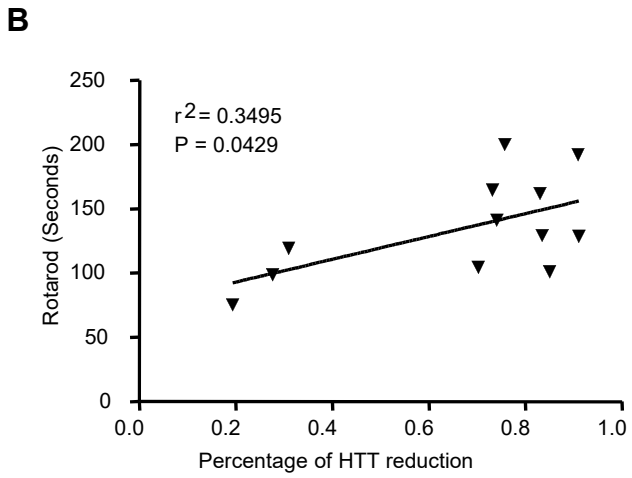
B
r 2 = 0.3495
P = 0.0429
Rotarod (Seconds)
250
200
150
100
50
0
0.0
0.2
0.4
0.6
0.8
1.0
Percentage of HTT reduction

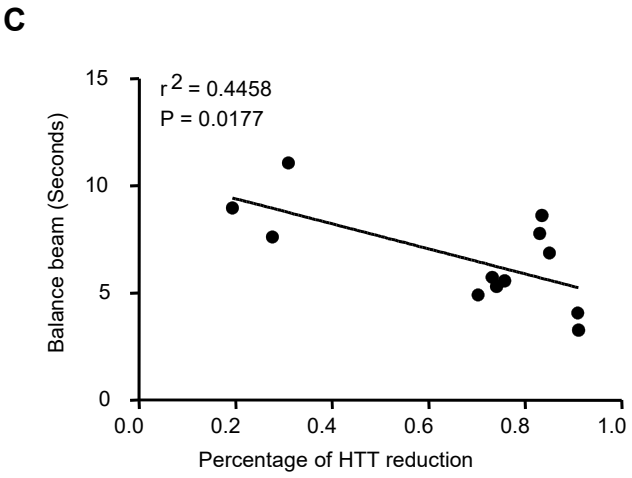
C
r 2 = 0.4458
P = 0.0177
Balance beam (Seconds)
15
10
5
0
0.0
0.2
0.4
0.6
0.8
1.0
Percentage of HTT reduction

Supplemental Figure 5. Correlation between mutant HTT reduction and behavioral performance (related to Figure 2).

(A) Western blotting analysis showing various levels of mutant HTT (mHTT) in the striatum of individual heterozygous HD140Q KI mice injected with AAV-Htt-gRNA/AAV-Mecp2-Cas9. The striatum of heterozygous HD140Q KI mice injected with AAV-Control-gRNA/AAV-Mecp2-Cas9 was used as a control.

(B) Lineal regression analysis correlating the percentage of mHTT reduction with rotorod performance in each individual heterozygous HD140Q KI mice injected with AAV-Htt-gRNA/AAV-Mecp2-Cas9 (n = 12).

(C) Lineal regression analysis correlating the percentage of mHTT reduction with balance beam performance in each individual heterozygous HD140Q KI mice injected with AAV-Htt-gRNA/AAV-Mecp2-Cas9 (n = 12).

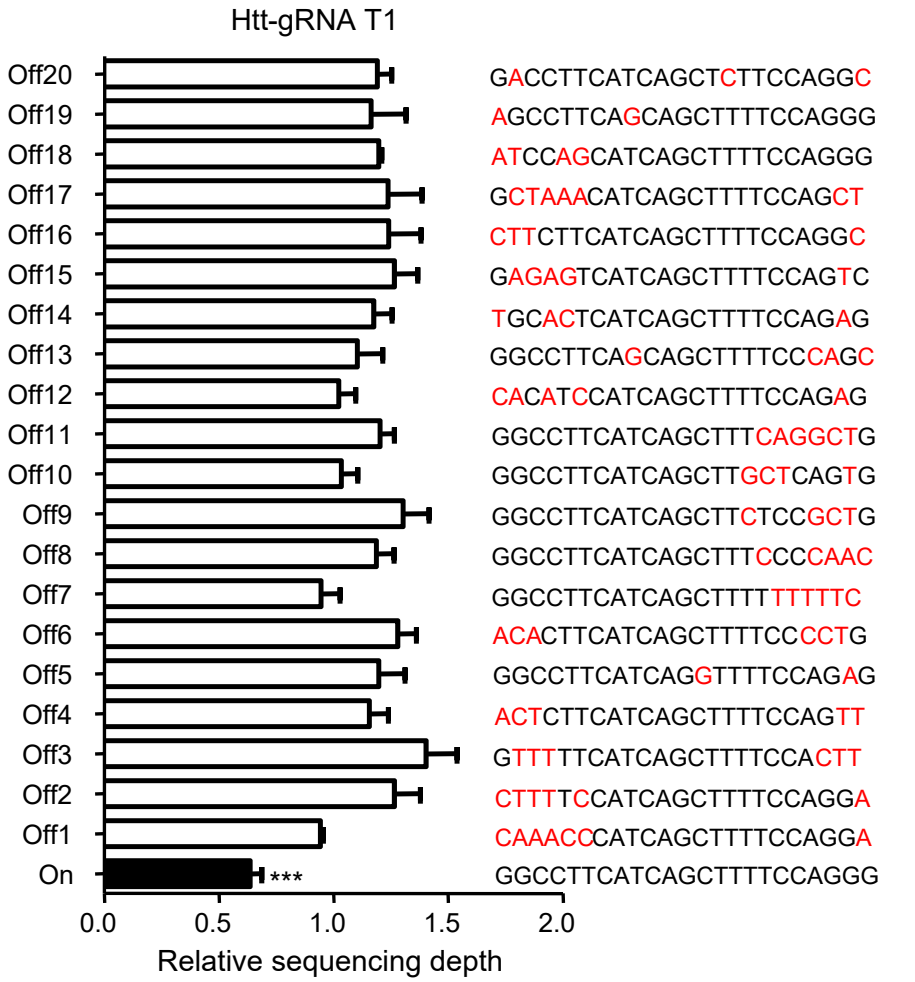
Htt-gRNA T1
Off20
Off19
Off18
Off17
Off16
Off15
Off14
Off13
Off12
Off11
Off10
Off9
Off8
Off7
Off6
Off5
Off4
Off3
Off2
Off1
On
***
GACCTTCATCAGCTCTTCCAGGC
AGCCTTCAGCAGCTTTTCCAGGG
ATCCAGCATCAGCTTTTCCAGGG
GCTAAACATCAGCTTTTCCAGCT
CTTCTTCATCAGCTTTTCCAGGC
GAGAGTCATCAGCTTTTCCAGTC
TGCACTCATCAGCTTTTCCAGAG
GGCCTTCAGCAGCTTTTCCCAGC
CACATCCATCAGCTTTTCCAGAG
GGCCTTCATCAGCTTTCAGGCTG
GGCCTTCATCAGCTTGCTCAGTG
GGCCTTCATCAGCTTCTCCGCTG
GGCCTTCATCAGCTTTCCCCAAC
GGCCTTCATCAGCTTTTTTTTTC
ACACTTCATCAGCTTTTCCCCTG
GGCCTTCATCAGGTTTTCCAGAG
ACTCTTCATCAGCTTTTCCAGTT
GTTTTTCATCAGCTTTTCCACTT
CTTTTCCATCAGCTTTTCCAGGA
CAAACCCATCAGCTTTTCCAGGA
GGCCTTCATCAGCTTTTCCAGGG
0.0
0.5
1.0
1.5
2.0
Relative sequencing depth

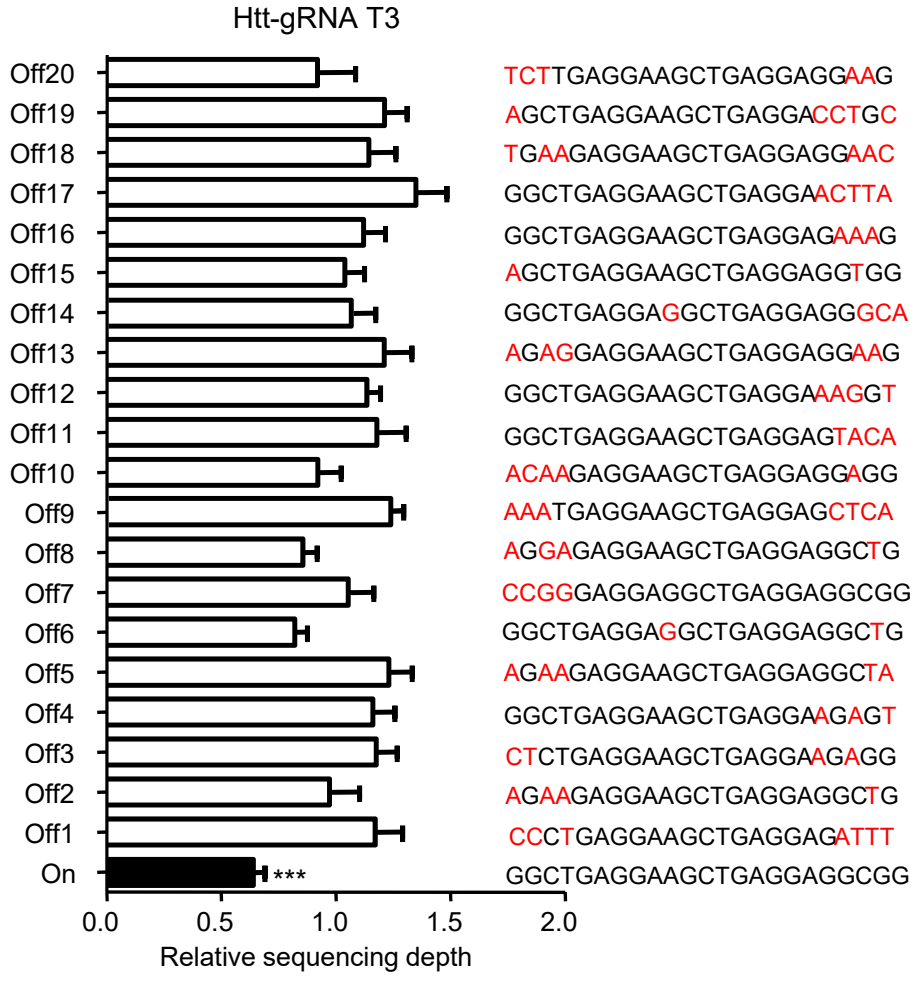
Htt-gRNA T3
Off20
Off19
Off18
Off17
Off16
Off15
Off14
Off13
Off12
Off11
Off10
Off9
Off8
Off7
Off6
Off5
Off4
Off3
Off2
Off1
On
***
TCTTGAGGAAGCTGAGGAGGAAG
AGCTGAGGAAGCTGAGGACCTGC
TGAAGAGGAAGCTGAGGAGGAAC
GGCTGAGGAAGCTGAGGAACTTA
GGCTGAGGAAGCTGAGGAGAAAG
AGCTGAGGAAGCTGAGGAGGTGG
GGCTGAGGAGGCTGAGGAGGGCA
AGAGGAGGAAGCTGAGGAGGAAG
GGCTGAGGAAGCTGAGGAAAGGT
GGCTGAGGAAGCTGAGGAGTACA
ACAAGAGGAAGCTGAGGAGGAGG
AAATGAGGAAGCTGAGGAGCTCA
AGGAGAGGAAGCTGAGGAGGCTG
CCGGGAGGAGGCTGAGGAGGCGG
GGCTGAGGAGGCTGAGGAGGCTG
AGAAGAGGAAGCTGAGGAGGCTA
GGCTGAGGAAGCTGAGGAAGAGT
CTCTGAGGAAGCTGAGGAAGAGG
AGAAGAGGAAGCTGAGGAGGCTG
CCCTGAGGAAGCTGAGGAGATTT
GGCTGAGGAAGCTGAGGAGGCGG
0.0
0.5
1.0
1.5
2.0
Relative sequencing depth

Supplemental Figure 6. Whole genome sequencing analysis showing rare off-target mutations in the striatum injected with AAV-Htt-gRNA/AAV-Mecp2-Cas9 (related to Figure 2).

Genomic DNAs from the striatum of mice injected with AAV-Htt-gRNA/AAV-Mecp2-Cas9 were subjected to whole genome sequencing. Relative sequencing depth for the *Htt* locus targeted by Htt-gRNAs (T1 and T3) and 20 most likely off-target loci was calculated by normalizing the number of mapped reads in those loci to the genome-wide average of mapped reads. Mutations caused by Cas9 cutting led to a reduce number of mapped reads, thereby a reduced relative sequencing depth. Relative sequencing depth for the *Htt* locus, but not the off-target loci, was significantly decreased (n = 4, one way ANOVA with Tukey tests, *** $P < 0.001$).

A

	Potential off-targets	Matching sequence
1	Hivep3, transcript variant X6	CCCTGGAAAAGC TGA
2	Hivep3	CCATGGAAAAGC TGA
3	Snrnp70, transcript variant X4	CCCTGGAAAAGC TG

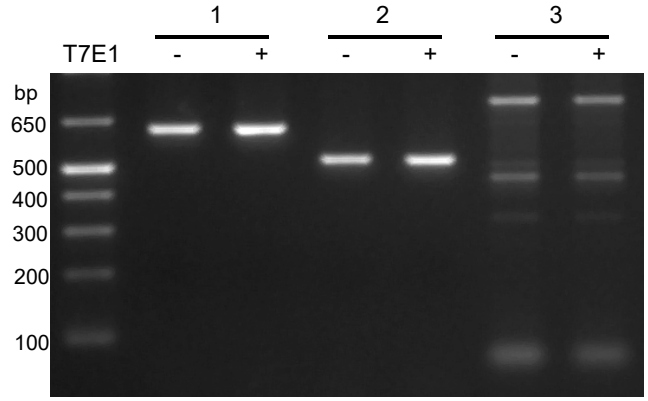

B

	Potential off-targets	Matching sequence
1	F-box/LRR-repeat protein 17	CCCCCTCCTCAG GTTCCTCA
2	tubulin beta-4B chain	CCTCCTCCTCAG CCTCCTC
3	Zfp865, transcript variant X4	CCGCCTCCTCA GCCTCCTC

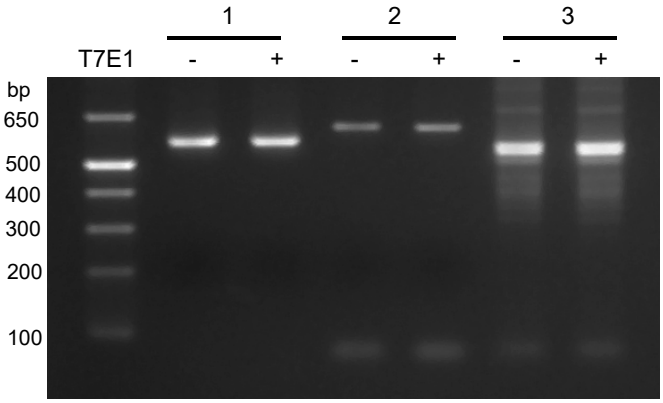

C

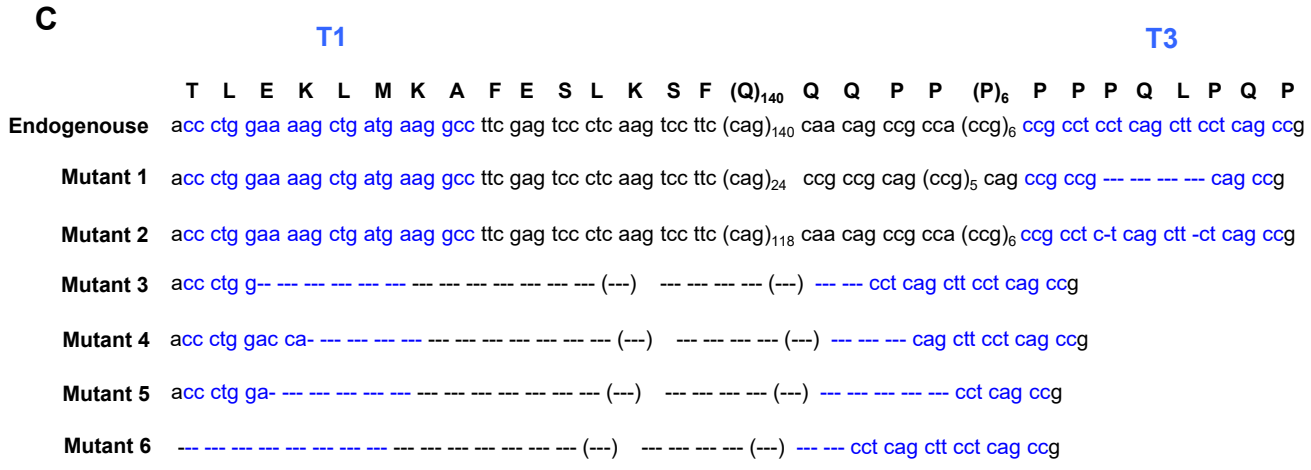

Supplemental Figure 7. Further analysis of genomic mutations in the striatum injected with AAV-Htt-gRNA/AAV-Mecp2-Cas9 (related to Figure 2).

(A, B) Three potential off-target loci (upper panel) for Htt-gRNA T1 (A) and T3 (B) were amplified by PCR, and examined by T7E1 assay. No DNA mutations were revealed

(C) Sequencing results of *Htt* genomic locus targeted by Htt-gRNAs. Six representative mutant sequences after Cas9 cutting were shown, Htt-gRNA T1 and T3 sequences were highlighted in blue.

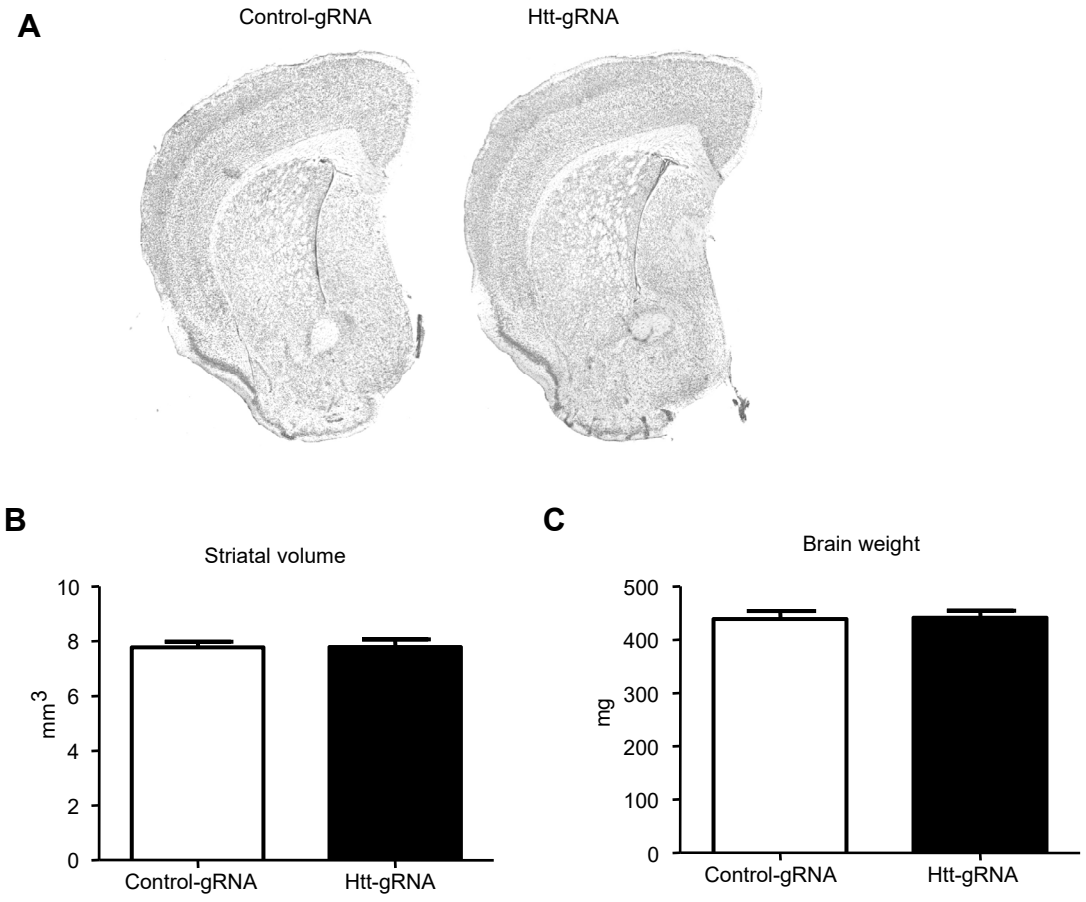
A
Control-gRNA
Htt-gRNA
B
Striatal volume
mm3
10
8
6
4
2
0
Control-gRNA
Htt-gRNA
C
Brain weight
mg
500
400
300
200
100
0
Control-gRNA
Htt-gRNA

Supplemental Figure 8. Examination of striatal volume and brain weight of heterozygous HD140Q KI mice injected with AAV-Htt-gRNA/AAV-Mecp2-Cas9 (related to Figure 3).

(A) Nissl staining result of brain sections from heterozygous HD140Q KI mice injected with either AAV-Htt-gRNA/AAV-Mecp2-Cas9 or AAV-Control-gRNA/AAV-Mecp2-Cas9.

(B) Quantitative analysis of striatal volume in heterozygous HD140Q KI mice injected with either AAV-Htt-gRNA/AAV-Mecp2-Cas9 or AAV-Control-gRNA/AAV-Mecp2-Cas9 (n = 8, Student's t-test).

(C) Quantitative analysis of brain weight of heterozygous HD140Q KI mice injected with either AAV-Htt-gRNA/AAV-Mecp2-Cas9 or AAV-Control-gRNA/AAV-Mecp2-Cas9 (n = 8, Student's t-test).